ICES Journal of Marine Science

ICES Journal of Marine Science (2016), 73(8), 1955–1964. doi:10.1093/icesjms/fsw055

Contribution to the Symposium: '*Marine Acoustics Symposium*'

Original Article

Optimizing transmit interval and logging range while avoiding aliased seabed echoes

Josiah S. Renfree* and David A. Demer

Southwest Fisheries Science Center, 8901 La Jolla Shores Drive, La Jolla, CA 92037, USA

**Corresponding author: tel: +1 858 546 5669; fax: +1 858 546 5656; e-mail: josiah.renfree@noaa.gov*

Renfree, J. S., and Demer, D. A. Optimizing transmit interval and logging range while avoiding aliased seabed echoes. – ICES Journal of Marine Science, 73: 1955–1964.

Received 9 October 2015; revised 5 February 2016; accepted 14 March 2016; advance access publication 21 April 2016.

Echosounder surveys of fish and zooplankton are typically conducted using fixed values of the echosounder transmit-pulse ("ping") interval and data-logging range. The transmit-pulse interval must be long enough to sample to the range of the farthest (deepest) species under study, potentially causing undersampling of closer (shallower) species. We present an algorithm to dynamically minimize both the logging range and transmit-pulse interval while ensuring that the logging range equals or exceeds the range to the seabed up to a chosen maximum data-logging range. The algorithm also allows avoidance of aliased seabed echoes ("false bottoms") by adjusting the minimized transmit interval such that seabed reverberation from a previous transmission is not present in the data logged for an ensuing transmission. Additionally, periodic measures of ambient noise allow evaluations of signal quality and useful range. This optimization scheme ("adaptive logging") effectively increases the horizontal resolution and signal-to-noise ratio of the data, and may reduce the total data volume and storage-space requirement. The efficacy of the adaptive logging algorithm is quantified using simulations. Furthermore, an example implementation of the algorithm is demonstrated for a commonly used scientific echosounder (Simrad EK60).

Keywords: adaptive logging, adaptive sampling, bottom detection, echosounder, ecosystem approach, false bottom.

Terms, symbols, and units

Term	Symbol	Unit	Description
Transmit-pulse interval	I_T	Second (s)	Time between consecutive pulse transmissions.
Minimum transmit-pulse interval	$I_{T\ min}$	s	The minimum achievable transmit-pulse interval.
Data-logging range	R_L	m	Range to which data are logged.
Maximum data-logging range	$R_{L\ max}$	m	The maximum distance from the transducer for which data will collected.
Seabed range	R_S	m	Distance from the transducer to the seabed.
Estimated seabed range	$\widehat{R_S}$	m	Estimated distance from the transducer to the seabed.
Continuous observation range	R_{CO}	m	Distance from the transducer at which the conical beams from successive transmissions begin to overlap.
Seabed offset range	R_0	m	Range beyond $\widehat{R_S}$ for which data are to be collected.
Aliased seabed echo range	R_{AS}	m	Distance at which the aliased seabed echoes appear in the data received for the present transmission.
Echogram-display range	R_D	m	Range to which received acoustic data are displayed on an echogram.
Seabed detection range	R_{SD}	m	Maximum distance evaluated for the seabed echo.
Data subscription range	R_{DS}	m	Distance for which sample data are obtained.

Continued

Continued

Term	Symbol	Unit	Description
Evaluation range	R_E	m	Distances evaluated for the seabed echo.
Detection search margin	Δ	m	Distance above the previously detected seabed depth for which ensuing detections will begin.
Evaluation range step	Δr	M	Distance that R is increased when $\widehat{R_S}$ is not detected.
Nearfield range	R_{NF}	M	Distance of the first Fresnel zone from the transducer.
Sound speed	c	m s^{-1}	Distance sound travels in water per unit time.
Echosounder sampling interval	F_S	s $sample^{-1}$	Time between digital samples.
Transmit pulse duration	τ	S	Duration of a signal pulse.
Absorption coefficient	α_a	dB m^{-1}	Frequency-dependent reduction in acoustic intensity with range, resulting from conversion to heat.
On-axis gain	G_O	dB re 1	Echosounder gain on the transducer beam axis.
Equivalent two-way beam angle	ψ	dB re 1 steradian	Solid angle subtended by an ideal conical beam that would produce the same volume integral as the square of the normalized transducer directivity.
S_A correction factor	$S_{A\ corr}$	dB re 1 m^{-1}	Factor used to account for effects of the echosounder receiver filter.
Directional angles	α,β	Degree (°)	Angle coordinates in orthogonal planes, typically alongships and athwartships or aligned with the major and minor transducer axes, respectively.
Transducer angle sensitivity	$\Lambda\alpha$ or $\Lambda\beta$	Electrical°/geometric°	Factor to convert split-beam electrical angles to target bearing angles in the α or β planes.
Transmit power	p_{et}	W	The electric power input to a transducer.
Received power	p_{er}	dB re 1 W	Root-mean-square (rms) received energy per unit time.
Noise power	p_{en}	dB re 1 W	P_{er} resulting from ambient noise.
Volume-backscattering coefficient or Volume-backscattering strength	s_V or S_V	m^{-1} or dB re 1 m^{-1}	Sum of acoustic backscattering cross section per unit of water volume.
Filtered S_V	$S_{V\ filt}$	dB re 1 m^2 m^{-3}	S_V filtered with a moving average.
Ambient noise S_V	$S_{V\ noise}$	dB re 1 m^2 m^{-3}	S_V resulting from the ambient P_{en}
Area backscattering coefficient or Nautical-area backscattering coefficient	s_a or S_A	m^2 m^{-2} or m^2 nautical $mile^{-2}$	The integral of S_V over a range of depths; or S_a multiplied by a unit-conversion factor [$4\pi(1852)^2$ nautical $mile^2$ m^{-2}]
Surface backscattering strength	S_s	dB re 1 m^2 m^{-2}	Backscattering cross section per unit of surface area.
Echo amplitude	e	Pa	Proportional to the square root of S_V.
Variance-to-mean ratio	No symbol	dB re 1	Ratio of the variance and mean of the estimated e.
Horizontal speed	s	m s^{-1}	Distance travelled per unit time in the horizontal direction.
Signal-to-noise ratio (SNR)	No symbol	dB re 1	Signal power (dB re 1 W) minus P_{en}.
Acoustic frequency	f	Hz	Number of complete cycles of a periodic wave per unit time.
Echosounder processing time	T_P	S	Time needed to transfer, analyse, and log data.
Number of frequencies	N_f	Dimensionless	Number of echosounder frequencies used in the analysis.
Number of seabed echo reflections	n_0	Dimensionless	Number of reflections off the seabed before the initial seabed echo arrives at the emitting transducer.
Number of transmissions before current transmission	N_1	Dimensionless	Number of transmissions before the current transmission from which the initial seabed echo arrives at the emitting transducer.
Acoustic data volume	V_A	Bytes (B)	Total volume of recorded acoustic data.
Acoustic data volume rate	V_R	B $sample^{-1}$	Data volume for a single sample of acoustic data.
Transmission samples	S_n	Dimensionless	Number of data samples recorded following a pulse transmission.
Number of transmissions	N_t	Dimensionless	Number of pulse transmissions emitted during an analysis period.
Instantaneous volume rate	V_I	B s^{-1}	Size of acoustic data volume obtained per unit of time.
Cartesian distances	x, y, and z	m	Orthogonal distances resulting from coordinate transformation of target range and phase angle data.

Introduction

Transmit interval and logging range

Fisheries acoustic surveys are typically conducted with fixed values for the echosounder transmit-pulse ("ping") interval (I_T; s) and data-logging range (R_L; m), which are related to the sound speed (c; m s^{-1}),

$$I_T \geq 2R_L/c. \quad (1)$$

The value of R_L must exceed the maximum range (depth) of the target species. However, when the range to the seabed (R_S; m) is less than R_L, and data from ranges greater than R_S are not needed, then R_L and I_T become unnecessarily large. For example, if $c = 1500$ m s^{-1} and $R_L = 750$ m, then $I_T \geq 1$ s; but if $R_S = 30$ m and $R_L = 40$ m, then $I_T \geq 0.05$ s, a nearly 20-fold decrease. Furthermore, for a conical, downwards-projecting transducer beam, its cross sectional area increases proportionally to the square of the observation range. When the transducer is moved at a speed (s; m s^{-1}), it travels distance

sI_T between each pulse transmission. At short ranges, the small insonified sample volumes of sequential transmissions are non-overlapping, but begin to overlap for ranges equal to or greater than the continuous observation range (R_{CO}; m) (Figure 1).

$$R_{CO} \geq \frac{sI_T}{2\tan(\theta/2)}. \quad (2)$$

In echo-integration processing, volume-backscattering coefficients (s_V; m^{-1}), which often range multiple orders of magnitude within an aggregation of sound scatterers, are summed over range (typically

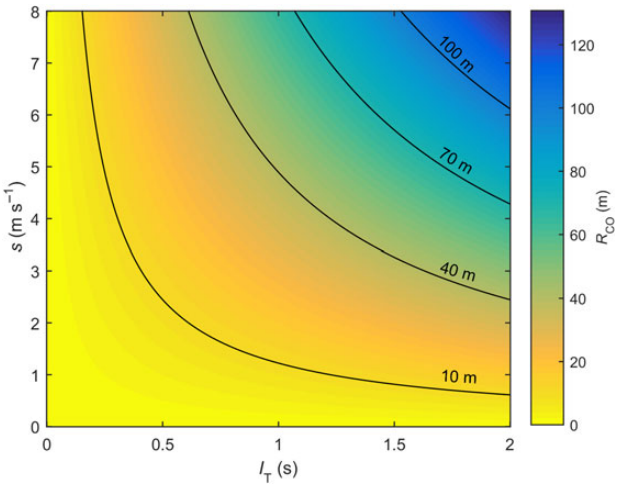

Figure 1. Continuous observation range (R_{CO}; m) vs. transmit-pulse interval (I_T; s) and ship speed (s; m s^{-1}) for a transducer with a 7° beam width. This figure is available in black and white in print and in colour at *ICES Journal of Marine Science* online.

depth) and averaged over the number of pulse-echoes in the analysis distance (e.g. Zwolinski *et al.*, 2014). The Law of Large Numbers indicates that the estimated mean will approach the true mean as the number of values (N) in the average approaches infinity; and the Central Limit Theorem indicates that the estimated means will be normally distributed with a variance proportional to $1/N$. Therefore, if transmissions are more frequent and the number of summed s_V values in the average is increased, the variance of the area backscattering coefficient (s_a; m^2m^{-2}) is reduced by a factor equal to the number of pulse-echoes, assuming the samples are independent. In general, it is beneficial to sample more frequently to minimize sampling uncertainty. If the sampled volumes from sequential transmissions overlap, the inter-sample correlation will increase but the higher spatial resolution may provide additional information, e.g. for patchily distributed targets such as epi-pelagic fish schools. Because R_{CO} is proportional to s and I_T, maximizing continuous observations may be achieved by reducing either value or both. If s is dictated by the weather, survey plan, or requisite survey-transect distance, then I_T, and therefore R_L, should be minimized.

The aim of this study is to develop an optimization ("adaptive logging") scheme that (i) dynamically minimizes both R_L and I_T while ensuring that $R_L > R_S$ until R_L equals a chosen maximum data-logging range ($R_{L\ max}$; m) and (ii) avoids noise from aliased seabed echoes (Figure 2), colloquially "false bottoms," by modulating the minimized I_T such that seabed reverberation from a previous transmission is not included in the data logged for an ensuing transmission. By meeting these objectives, this adaptive logging scheme will effectively increase the spatial and temporal resolutions, signal-to-noise ratio (SNR), and processing speed of the data while reducing the total data volume and storage-space requirement. The algorithms are particularly useful for surveys of multiple species that span a large range of depths (e.g. epi-pelagic to demersal species). Presented is an example of their implementation in

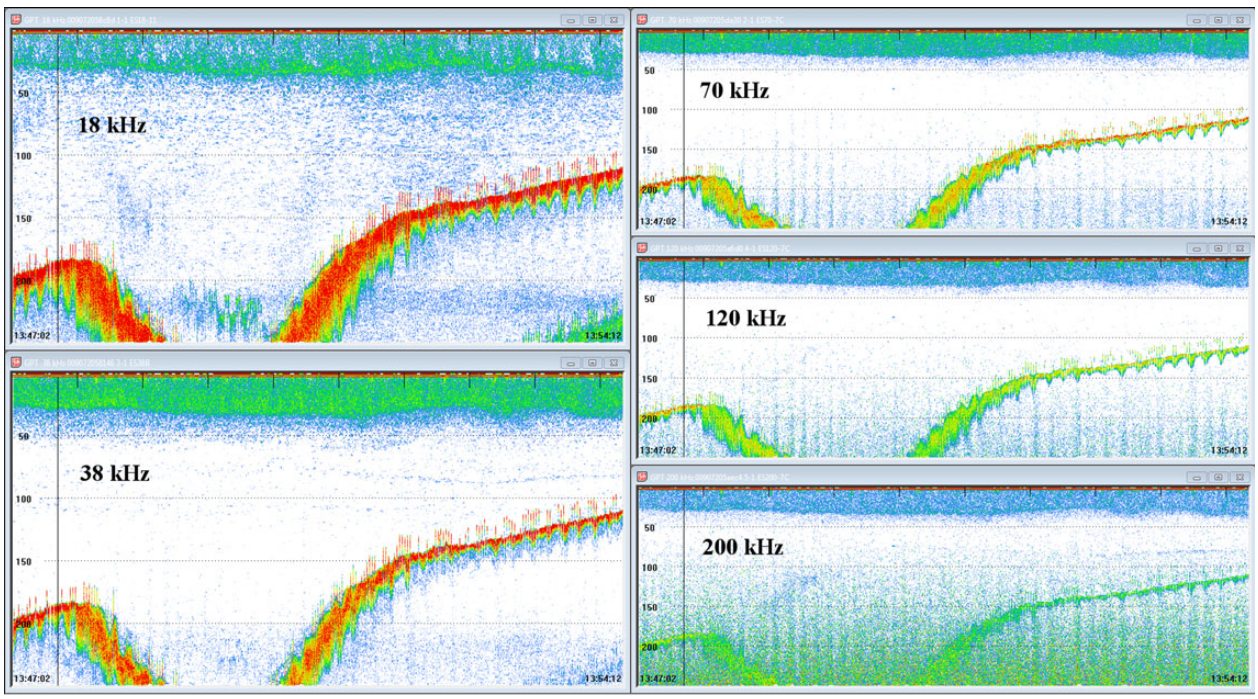

Figure 2. Echograms at 18, 38, 70, 120, and 200 kHz (top to bottom, from left to right) showing an aliased seabed echo ("false bottom"), characteristically decreasing in intensity with increasing frequency. Levels, light to dark, correspond to S_V from −70 to −34 dB. This figure is available in black and white in print and in colour at *ICES Journal of Marine Science* online.

software specific to a commonly used scientific echosounder (Simrad EK60). Although the software is specific to a split-beam transducer system, the optimization equations are generically applicable to single- and split-beam systems with one or more transducers.

Seabed detection

The first essential task in this scheme is to accurately and robustly estimate the range to the seabed ($\widehat{R}_S$; m). Echosounders typically calculate $\widehat{R}_S$ from the product of c and half the arrival time (to account for the two-way travel distance) of the maximum sample of single-frequency S_v. Although the arrival time may be compensated for receiver delay, echo rise-time, and signal quantization (Simmonds and MacLennan, 2005), the directivity and steering of the acoustic beam, rugosity of the seabed, and echoes from dense aggregations of fish or zooplankton can all cause high-intensity returns in advance of the echo from the seabed (Ona and Mitson, 1996; MacLennan *et al.*, 2004). Therefore, S_v-based $\widehat{R}_S$ are often biased with false positives (i.e. the seabed is incorrectly detected). Furthermore, if the SNR is low, this method may fail, resulting in false negatives (i.e. the seabed is incorrectly not detected). Alternatively, echo amplitudes and biplanar, split-beam phase data collected at multiple frequencies (f, Hz) may be used to more accurately and robustly calculate $\widehat{R}_S$ (Demer *et al.*, 2009; Cutter and Demer, 2010, 2014).

Aliased seabed echoes

Seabed echoes from a preceding transmission may arrive at the transducer during the reception period for the current transmission. When $I_T c/2 \leq R_S$, these seabed echoes arrive directly to the transducer. When $I_T c/2 \geq R_S$, these seabed echoes reflect off the sea surface and again off the seabed, one or more times, before arriving at the transducer. In either case, the aliased seabed echoes result in erroneous data, essentially noise, and thus a reduced SNR. This signal degradation may necessitate filtering and can result in false-positive seabed detections. In cases where aliased seabed echoes have appreciable intensity, particularly for the first or second echo at low frequencies, avoidance of the echoes may necessitate modulating I_T.

Generalized methods

Optimizing R_L and I_T

To minimize the collection of unusable data, R_L is dynamically chosen to exceed $\widehat{R}_S$ by an offset range (R_O; m) up to $R_{L\,max}$:

$$R_L = \min(R_{L\,max}, \widehat{R}_S + R_O), \tag{3}$$

where min() yields the smaller of the two operands. Depending on R_L and the processing time (T_P; s) needed for the echosounder to transfer, analyse, and log data from N_f echosounder frequencies, the minimum practicable transmit interval ($I_{T\,min}$; s) is:

$$I_{T\,min} = \frac{2R_L}{c} + T_P. \tag{4}$$

Aliased seabed echoes

Relative to the initial transmission time, and with ranges referenced to the sea surface, seabed echoes occur at positive integer-multiples (n_0) of $2R_S/c$ and decrease in intensity with increasing f, due to absorption losses (Francois and Garrison, 1982); increasing R_S and n_0, due to spreading losses; and decreasing surface backscattering strength (S_s; dB re 1 m^2 m^{-2}) of the seabed. The presence of aliased seabed echoes is, therefore, dependent upon R_S and I_T.

When $I_T c/2 > R_S$, aliased seabed echoes (Figure 3a) appear in the echosounder data at range R_{AS} (m):

$$R_{AS} = n_0 R_S - \frac{I_T c}{2}, \tag{5}$$

where n_0 is the smallest integer resulting in a positive R_{AS}:

$$n_0 = \left\lceil \frac{I_T c}{2R_S} \right\rceil. \tag{6}$$

where $\lceil\rceil$ yields the smallest integer greater than the operand (ceiling). Substituting Equation (6) into Equation (5) yields:

$$R_{AS} = \left\lceil \frac{I_T c}{2R_S} \right\rceil R_S - \frac{I_T c}{2}. \tag{7}$$

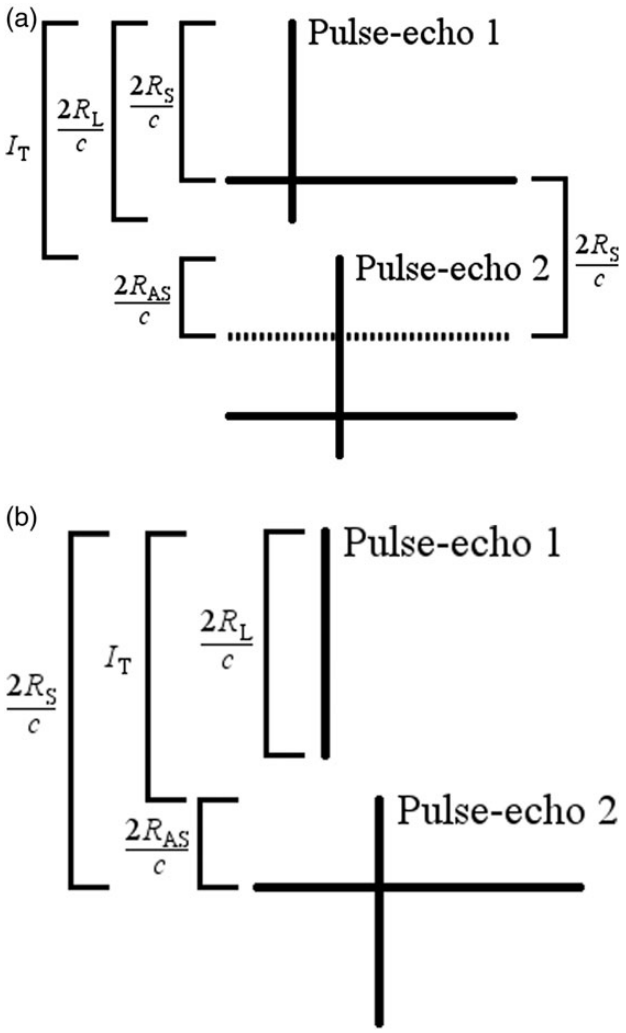

Figure 3. The relationships between the times associated with transmit pulses (solid vertical lines), logging range (R_L), transmit interval (I_T), range to the seabed (R_S), seabed echoes (solid horizontal lines), and the location of aliased seabed echoes (dotted or solid horizontal lines) when $2R_S/c$ is (a) less than I_T and (b) greater than I_T.

When $I_T c/2 \leq R_S$, aliased seabed echoes are caused by the first echo of the seabed from the n_1th previous transmission (Figure 3b), and similarly:

$$R_{AS} = R_S - n_1 \frac{I_T c}{2}, \tag{8}$$

$$n_1 = \left\lfloor \frac{2R_S}{I_T c} \right\rfloor, \tag{9}$$

and

$$R_{AS} = R_S - \left\lfloor \frac{2R_S}{I_T c} \right\rfloor \frac{I_T c}{2}, \tag{10}$$

where $\lfloor\rfloor$ yields the largest integer less than the operand (floor). In practice, the R_S in Equations (5)–(10) are replaced by its estimator, $\widehat{R_S}$.

Aliased seabed removal

Removal of aliased seabed echoes is only required if $R_{AS} \leq \min(\widehat{R_S}, R_{L\max})$. If substituting $I_{T\,\min}$ for I_T in Equations (7) or (10) results in this condition, a delay is added to $I_{T\,\min}$ such that the aliased seabed echo precedes the logging period. The minimum I_T resulting in no aliased seabed echo occurs when R_{AS} is equal to 0 m. If $I_T c/2 > \widehat{R_S}$, Equation (5) becomes

$$I_T = \frac{2n_0\widehat{R_S}}{c}. \tag{11}$$

Since $I_T \geq I_{T\,\min}$, n_0 is calculated as:

$$\begin{aligned} \frac{2n_0\widehat{R_S}}{c} &\geq I_{T\,\min}, \\ n_0 &\geq \frac{I_{T\,\min} c}{2\widehat{R_S}}, \quad \text{and} \\ n_0 &= \left\lceil \frac{I_{T\,\min} c}{2\widehat{R_S}} \right\rceil. \end{aligned} \tag{12}$$

If R_S is assumed to be constant, the n_0th seabed reflection results in the highest intensity aliased seabed echo for the next logging period. While transmissions before the n_0th seabed reflection could also result in aliased seabed echoes, the intensities would be negligible in comparison. Similarly, if $I_T c/2 < \widehat{R_S}$, and again forcing R_{AS} to equal 0 m, Equation (8) becomes:

$$I_T = \frac{2\widehat{R_S}}{n_1 c}, \tag{13}$$

$$\begin{aligned} \frac{2\widehat{R_S}}{n_1 c} &\geq I_{T\,\min}, \\ n_1 &\leq \frac{2\widehat{R_S}}{cI_{T\,\min}}, \quad \text{and} \\ n_1 &= \left\lfloor \frac{2\widehat{R_S}}{cI_{T\,\min}} \right\rfloor. \end{aligned} \tag{14}$$

Again, if R_S is assumed to be constant, the n_1th previous transmission results in the strongest aliased seabed echo. If I_T is chosen such that R_{AS} equals 0 m, then R_{AS} will continue to be 0 m for all future transmissions. In reality, R_S is rarely constant, and extremely abrupt or drastic changes in R_S can result in the reappearance of aliased echoes, but generally the variability in R_S is negligible, especially when optimizing I_T.

To summarize, R_{AS} is first estimated from Equations (7) or (10) with I_T equal to $I_{T\,\min}$, and the new I_T calculated by:

$$I_T = \begin{cases} I_{T\,\min}; & R_{AS} \geq \min(\widehat{R_S},\ R_{L\,\max}) \\ \dfrac{2n_0\widehat{R_S}}{c},\ n_0 = \left\lceil \dfrac{I_{T\,\min} c}{2\widehat{R_S}} \right\rceil; & R_{AS} < \min(\widehat{R_S},\ R_{L\,\max}) \text{ and } \dfrac{I_T c}{2} > \widehat{R_S} \\ \dfrac{2\widehat{R_S}}{n_1 c},\quad n_1 = \left\lfloor \dfrac{2\widehat{R_S}}{cI_{T\,\min}} \right\rfloor; & R_{AS} < \min(\widehat{R_S},\ R_{L\,\max}) \text{ and } \dfrac{I_T c}{2} < \widehat{R_S} \end{cases}. \tag{15}$$

Generalized results

I_T and R_L distributions

Using adaptive logging and Equations (4) and (15), benchmark relationships are shown for I_T vs. R_S, with and without removal of aliased seabed echoes, assuming $c = 1500$ m s^{-1}, $R_{L\,\max} = 700$ m, $T_P = 0.07$ s, and $R_O = 60$ m (Figure 4). If aliased seabed echoes are not removed, either $R_S < R_{L\,\max} - R_O$ and I_T increases linearly with R_L or $R_S \geq R_{L\,\max} - R_O$ and I_T increases by T_P. If $R_{AS} \leq \min(R_S, R_{L\,\max})$, aliased seabed echoes may be removed, in which case the sampling resolution may decrease due to the delay required for excluding the aliased echoes from ensuing transmissions. The delay added to $I_{T\,\min}$ is limited to the time equivalent of R_S (i.e. $2R_S/c$) and is maximal when $R_{AS} = R_{L\,\max}$ (i.e. $2R_{L\,\max}/c$). Again, in practice, R_S are replaced by $\widehat{R_S}$.

Data volume

Adaptive sampling eliminates the unnecessary collection of data beyond the time equivalent of $\widehat{R_S} + R_O$ (i.e. $2(\widehat{R_S} + R_O)/c$) when $\widehat{R_S} < R_{L\,\max}$. The volume of data collected (V_A; bytes) depends on the data rate (V_R; bytes sample^{-1}), the number of samples from the

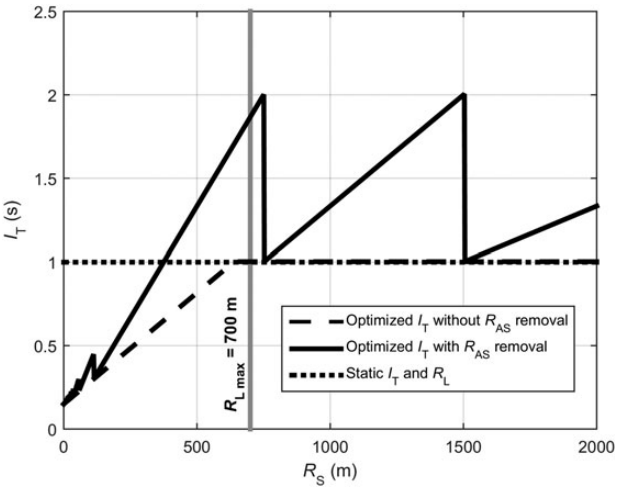

Figure 4. Relationship between I_T and R_S with either fixed logging settings (dotted line), adaptively sampling but without removing aliased seabed echoes (dashed line), or adaptively sampling and removing aliased seabed echoes (solid line). In this example, $R_{L\,max} = 700$ m, $c = 1500$ m s^{-1}, $T_p = 0.07$ s, $R_O = 60$ m, and the static $I_T = 1.0$ s.

nth transmission (S_n), the number of transmissions (N_t), and N_f:

$$V_A = V_R N_f \sum_{n=1}^{N_t} S_n. \quad (16)$$

Rewriting Equation (16) in terms of R_L:

$$S_n = \frac{2R_L}{cF_S}, \quad (17)$$

where F_S is the echosounder sample interval (s sample^{-1}). Substituting Equation (17) into Equation (16) and rearranging:

$$V_A = \frac{2V_R N_f}{cF_S} \sum_{n=1}^{N_t} R_{L_n}. \quad (18)$$

Unlike V_A, which depends on N_t, the instantaneous rate at which data are generated for a single transmission (V_I; bytes s^{-1}) is a function of I_T:

$$V_I = \frac{2V_R N_f R_L}{cF_S I_T}. \quad (19)$$

V_I depends on I_T and R_L (Equation 19) and changes vs. R_S (Figure 5). Therefore, as seen in Equation (19), any reduction in R_L, increase in I_T, or both, will decrease V_I. The associated decrease in N_t would decrease V_A, as indicated in Equation (18).

Application methods

We applied our adaptive logging algorithm for optimizing I_T and R_L while avoiding aliased seabed echoes to a commonly used scientific echosounder (Simrad EK60) and software (Simrad ER60). Implemented in Matlab (Mathworks, Natick, MA, USA), the ER60 Adaptive Logger software (EAL) uses an Ethernet connection to the ER60 operating computer and the Remoting and Data Subscription protocol (see Simrad, 2012) to: (i) obtain User Datagram Protocol (UDP) packets containing received power [$P_{er}(f)$; dB re 1 W], alongships and athwartships phases, $S_v(f)$, and ambient noise power estimates [$P_{en}(f)$; dB re 1 W]; (ii) calculate $\widehat{R_S}$ and R_{AS} to optimize I_T; and (3) set echosounder parameters.

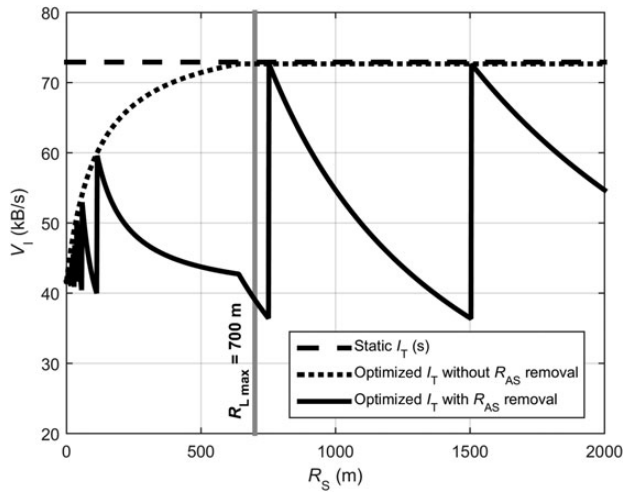

Figure 5. Comparison of the data volume rate (V_I) vs. seabed depth (R_S) when the echosounder is operated with static values of R_L and I_T (dashed line), and when the values of R_L and I_T are dynamically optimized using Equation (15), with (solid line) and without (dotted line) removal of aliased seabed echoes. In this example, $R_{L\,max}$ = 700 m, c = 1500 m s^{-1}, T_P = 0.07 s, R_O = 60 m, N_f = 5, F_S = 256 μs sample^{-1}, V_R = 4 bytes sample^{-1}, and the static I_T = 1.0 s.

EAL initialization

When started and stopped, the EAL sets the ER60 logging, display [$R_D(f)$; m], and seabed detection [$R_{SD}(f)$; m] ranges to the user-defined $R_{L\,max}$, changes the ER60 transmit mode to "interval," then calculates and sets I_T using $R_L = R_{L\,max}$ and Equation (4). The values of $R_{L\,max}$ and T_P are defined in a text file which is read and updated upon both startup and during the processing of each transmission. If the value of T_P is set too low, the ER60 will warn that the transmit-pulse interval cannot be achieved, in which case T_P should be incrementally increased until the warning ceases. Because values of R_L, $R_D(f)$, and $R_{SD}(f)$ all directly limit I_T, and I_T is calculated from R_L, the EAL maintains the values of $R_D(f) \leq R_L$ and $R_{SD}(f) \leq R_L$. This assures that the minimum achievable I_T is not affected if the values of R_L, $R_D(f)$, and $R_{SD}(f)$ are changed manually in the ER60. The EAL also reads values of c; pulse duration [$\tau(f)$; s]; absorption coefficient [$\alpha_a(f)$; dB m^{-1}]; transmit power [$p_{et}(f)$; W]; on-axis gain [$G_o(f)$; dB]; equivalent two-way beam angle [$\psi(f)$; dB]; S_A correction factor [$S_{A\,corr}(f)$; dB]; and alongships and athwartships angle sensitivities [$\Lambda_\alpha(f)$ and $\Lambda_\beta(f)$ electrical °/geometric°] for converting the split-beam phase data to $\alpha(f)$ and $\beta(f)$, respectively (see Demer *et al.*, 1999). These values are used by the EAL for estimating R_S.

Data acquisition

The EAL constantly reads UDP packets containing $P_{er}(f)$, alongships and athwartships phases, and $S_V(f)$ over a data subscription range (R_{DS}; m) spanning $0 < R_{DS} < R_L$. Furthermore, to calculate SNR vs. acoustic frequency and observation range, the EK60 transceivers are periodically operated in "passive mode" and the median $P_{en}(f)$ is recorded from multiple receptions. The ER60 calculates $P_{en}(f)$ by taking the median of 20 equidistant P_{er} samples spanning R_L (Lars Andersen, pers. comm., 14 May 2015). To ensure that all the data for each variable originate in the same transmission, the EAL evaluates the timestamps in each datagram. Incomplete sets are discarded and new data are subsequently read.

Evaluation ranges

It is assumed that R_S is always beyond the maximum nearfield range (R_{NF}; m) of the multifrequency transducers ($R_S > R_{NF}$). To mitigate spurious false-positive $\widehat{R_S}$, the following strategy is used to maintain the seabed within an evaluation range (R_E; m). Initially (Case 1), R_E spans $R_{NF} < R_E < R_{L\,max}$. If the seabed is not detected within this evaluation range for the first X transmissions (e.g. $X = 10$ to avoid false negatives), then it is assumed that $R_S > R_{L\,max}$ and the evaluation range for the next transmission (Case 2) spans $R_{L\,max} - \Delta R \leq R_E \leq R_{L\,max}$, where ΔR (m) is a search margin (e.g. 10 m) and $R_L = R_{L\,max}$. When $R_S < R_{L\,max}$ and R_S is contained in R_E (Case 3), $\widehat{R_S}$ is then used to update R_L according to Equation (3). The evaluation range is then updated such that:

$$\lfloor \max(R_{NF}, \widehat{R_S} - \Delta R) \rfloor \leq R_E \leq R_L \quad (20)$$

where max( ) yields the larger of the two operands. If the seabed is not detected, ΔR is increased by Δr (e.g. 5 m) for each ith successive transmission until either the seabed is detected and i resets to 0 or $\widehat{R_S} - \Delta R - i\Delta r \leq R_{NF}$ and R changes to Case 1.

Estimating R_S and R_{AS}

To estimate $\widehat{R}_S$, vectors of $S_V(f)$ are filtered using a 3-m simple moving average, resulting in smoothed samples of volume backscatter [$S_{Vfilt}(f)$; dB re 1 m^{-1}]. After converting $P_{en}(f)$ to volume backscatter [$S_{Vnoise}(f)$] (see Demer *et al.*, 2015), $S_{Vfilt}(f)$, $\alpha(f)$, and $\beta(f)$ are then noise-filtered by removing all samples for which $S_{Vnoise}(f) > -60$ dB. Samples of $S_{Vfilt}(f)$ within the current evaluation range (Table 1) are then converted to values proportional to echo amplitude ($e \propto 10^{S_{V\,filt}/20}$) and the variance-to-mean ratio (VMR) is calculated from e using samples from at least three frequencies (see Demer *et al.*, 2009). Samples with $\min(S_{Vfilt}(f)) > -50$ dB and VMR not less than -30 dB are deemed candidate seabed samples, which ensures SNR ≥ 10 dB and allows for detection of the seabed even when the VMR cannot be derived (e.g. low SNR). If no samples meet these criteria, R_S is considered unknown and the evaluation range expands until the Case 1 criteria are met. Otherwise, the seabed is located by finding $\max(S_{Vfilt}(f))$ within the candidate samples. Samples of the seabed echo are defined where $S_{Vfilt}(f)$ is greater than -50 dB on either side of the maximum-S_{Vfilt} seabed sample. If angular data are available (e.g. split-beam transducer), values of $\alpha(f)$ and $\beta(f)$ from the seabed echo are then converted to Cartesian distances [$x(f)$, $y(f)$, and seabed depth $z(f)$; m)](Conti *et al.*, 2005),

$$\begin{bmatrix} x(f) \\ y(f) \\ z(f) \end{bmatrix} = \frac{R(f)}{\sqrt{1 - \sin^2(\alpha(f))\,\sin^2(\beta(f))}} \begin{bmatrix} \sin(\alpha(f))\cos(\beta(f)) \\ \cos(\alpha(f))\sin(\beta(f)) \\ \cos(\alpha(f))\,\cos(\beta(f)) \end{bmatrix}, \tag{21}$$

and fit to a plane (Demer *et al.*, 2009):

$$z(f) = a(f)x(f) + b(f)y(f) + \widehat{R}_S(f). \tag{22}$$

For each f, the plane is fit using least-squares regression, linear matrix algebra, and Equation (22),

$$z(f) = \begin{bmatrix} x(f) & y(f) & 1 \end{bmatrix} \begin{bmatrix} a(f) \\ b(f) \\ \hat{R}_S(f) \end{bmatrix}, \tag{23}$$

$$\begin{bmatrix} a(f) \\ b(f) \\ \hat{R}_S(f) \end{bmatrix} = ([x(f) \quad y(f) \quad 1]^T [x(f) \quad y(f) \quad 1])^{-1} \begin{bmatrix} x(f) \\ y(f) \\ 1 \end{bmatrix} z(f),$$

where $x(f)$, $y(f)$, and $z(f)$ are column vectors, super script T signifies matrix transposition, and -1 indicates matrix inversion. If $[x(f)\ y(f)\ 1]^T[x(f)\ y(f) 1]$ results in a singular matrix, the data are deemed unsuitable for a plane fit and $\widehat{R}_S(f)$ is calculated as the mean of $z(f)$. Otherwise, $a(f)$ and $b(f)$ are used to estimate metrics of seabed slope and roughness (Demer *et al.*, 2009). In either case, $\widehat{R}_S$ is then calculated by averaging across $\widehat{R}_S(f)$. In the infrequent event that a fish-school echo within R_E is detected as the seabed (false positive), $\widehat{R}_S$ will track the school until it moves outside the acoustic beam, after which R_E will expand until $\widehat{R}_S$ is accurate.

When $R_S < R_L$ and $\widehat{R}_S$ can be directly estimated, $I_T c/2 > \widehat{R}_S$ and R_{AS} is calculated using Equation (7). When $R_S > R_{L\,max}$, either (i) R_L and I_T are periodically and temporarily increased such that $R_S < R_L$ and $\widehat{R}_S$ can be directly estimated or (ii) the echosounder location, estimated by a GPS receiver, is used to reference $\widehat{R}_S$ from a bathymetry database (e.g. a digital elevation model from Marine Geoscience Data System), interpolated within a longitude-latitude-depth grid spanning the survey region. Then, if $\frac{I_T c}{2} > \widehat{R}_S$ or $\frac{I_T c}{2} < \widehat{R}_S$, R_{AS} is calculated using Equation (7) or (10), respectively.

Calculating I_T

If the EAL is not configured to remove aliased seabed echoes, I_T is set equal to $I_{T\,min}$ as defined in Equation (4). Alternatively, if aliased seabed echoes are to be removed and $I_{T\,min}$ results in $R_{AS} \leq \min(\widehat{R}_S,\ R_{L\,max})$, I_T is calculated according to Equation (15). The EAL then sets I_T and R_L, changes $R_D(f)$ and $R_{SD}(f)$ to be equal to R_L, and updates R_{DS} to span $0 < R_{DS} < R_L$.

Application results

The adaptive logging algorithm is contingent on seabed depth, which is either detected or referenced from a database. To quantify the effectiveness of the EAL to robustly estimate R_S, optimize I_T and R_L, increase spatial resolution, decrease data volume, and eliminate aliased seabed echoes, data from a five-frequency (18, 38, 70, 120, and 200 kHz) EK60 were analysed. These data were collected during one representative transect (50.45°N 128.10°W to 50.45°N 129.01°W) of the Southwest Fisheries Science Center's 2015 Summer Coastal Pelagic Species (CPS) survey, conducted aboard the FSV *Bell M. Shimada*. The transect spanned the variety of scatterers and depths encountered throughout the entire survey, including regions where $R_S \leq R_{L\,max}$ and $R_S > R_{L\,max}$.

I_T and R_L distributions

Without the EAL, the CPS survey would have been conducted using a fixed $R_L = 700$ m and $I_T = 1.0$ s. This value of I_T is compared with that achieved using the EAL (Figure 6). When $R_L \ll R_{L\,max}$, the EAL increased the temporal resolution over

Table 1. The logging (R_L, m) and evaluation ranges (R, m) are set depending on the algorithm state.

Case	Condition	Logging range	Evaluation range	True seabed location		
1	Startup	$R_L = R_{L\,max}$	$R_{NF} < R_E \leq R_{L\_max}$	$R_S < R_{L\,max}$ N/A	$R_S > R_{L\,max}$ N/A	$R_S < R_{L\,max}$ N/A
2	No seabed is detected	$R_L = R_{L\,max}$	$R_{L\,max} - \Delta R \leq R_E \leq R_{L\,max}$	$R_S > R_{L\,max}$ True negative	$R_S < R_{L\,max} - \Delta R$ False negative	$R_{L\,max} - \Delta R < R_S < R_{L\,max}$ False negative
3	Seabed is detected	$R_L = \lvert\min(R_{L\,max}, \widehat{R}_S + R_0)\rvert$	$\widehat{R}_S - \Delta R \leq R_E \leq R_L$, where $\widehat{R}_S - \Delta R = R_{NF}$ if $\widehat{R}_S - \Delta R < R_{NF}$	$R_S > R_{L\,max}$ False positive	$R_S < \widehat{R}_S - \Delta R$ False positive	$\widehat{R}_S - \Delta R < R_S < R_L$ True positive

Within R, samples deemed to be seabed echoes are either true positive (the seabed is present and detected) or false positive (the seabed is not present but it is detected). Aliased seabed echoes may cause false positives. When the seabed is not detected, the evaluation is either true negative (the seabed is not present and not detected) or false negative (the seabed is present but not detected). Noise may cause false negatives.

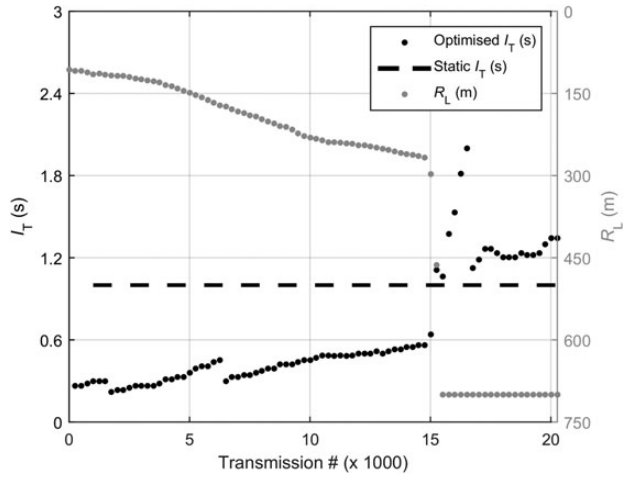

Figure 6. Comparison of I_T without (dashed black line) or with the EAL (black points) for one transect from the 2015 Summer CPS survey. The R_L (grey points) associated with each transmission is included for reference.

fourfold. However, the improvement in temporal resolution decreased as R_L approached $R_{L\,max}$.

Spatial resolution

The ~35-nautical mile transect was run at $s \approx 10$ kts. Without the EAL, a fixed $I_T = 1.0$ s would have resulted in a spatial resolution of ~360 transmissions per nautical mile. With the EAL, and with removal of aliased seabed echoes, data were collected from a total of 20 267 transmissions, resulting in an average spatial resolution of roughly ~579 transmissions per nautical mile for an improvement of 1.61 in the average spatial resolution. When $R_L \ll R_{L\,max}$, the increased sampling resolution due to the EAL (Figure 6) results in a corresponding increase in the spatial resolution of over fourfold. When $R_L \approx R_{L\,max}$, there was negligible or no improvement in spatial resolution.

Data volume

Throughout the transect, conducted with the EAL and with removal of aliased seabed echoes, a total of $N_t = 20\,267$ transmissions were collected using $N_f = 5$, $c = 1495.39$ m s^{-1}, and $F_S = 256$ μs sample^{-1}. Without the EAL, $I_T = 1.0$ s and $R_L = 700$ m, which would have resulted in $N_t = 12\,633$. Using Equation (18) with $V_R = 4$ (Simrad, 2012), V_A with and without the EAL was 670 MB and 924 MB, respectively, resulting in data volume savings of ~27%.

When $R_L < R_{L\,max}$: $V_A = 437$ MB without the EAL; and $V_A = 297$ MB with the EAL, for a data volume savings of ~32%. The EAL reduced V_A because it reduced V_I more than it increased N_t. When $R_L = R_{L\,max}$: $V_A = 487$ MB without the EAL; and $V_A = 373$ MB with the EAL and with removal of aliased seabed echoes, for a data volume savings of ~23%. Due to the removal of aliased seabed echoes, I_T with the EAL was generally greater than the static I_T of 1.0 s (Figure 6), resulting in a reduction of N_t and thus V_A.

Aliased seabed removal

With the EAL, aliased seabed echoes were removed when R_S was above and below $R_{L\,max}$. When $R_S \leq R_{L\,max}$, $\widehat{R}_S$ was measured directly. However, when $R_S \leq R_{L\,max}$, two more elaborate methods were utilized. The first method periodically and temporarily increased R_L to a large enough range (e.g. 5 km) to ensure $R_S < R_L$; then $\widehat{R}_S$ was measured directly, generally relying on data from the lower frequency echosounders. This $\widehat{R}_S$ was then used until either $R_S < R_{L\,max}$ or another periodic increase of R_L was performed (e.g. every 10 min), making the efficacy of this method dependent on the bathymetric variability between measurements. The second method utilized a bathymetry database for evaluating $\widehat{R}_S$ based on the current geographic location, which it used to estimate R_{AS} and remove aliased seabed echoes. The bathymetry database was not corrected for tide because the bias was negligible when $R_S < R_{L\,max}$, else $\widehat{R}_S$ was measured directly. Both methods of evaluating $\widehat{R}_S$ consistently removed aliased seabed echoes (Figure 7).

Discussion

Echo integration is based on the mean nautical-area backscattering coefficient (s_A; m^2 nautical mile^{-2}). Basic statistics theory indicates that when the number of observations of a population is small, it is likely that the estimated value is biased from the true value. Biased s_A values can affect the accuracy of both target classification and density estimation. Therefore, s_A for individual aggregations are more accurately and precisely estimated by maximizing the number of observations (Demer *et al.*, 2009), accomplished by optimally minimizing the transmit interval.

Historically, surveys of single species have been conducted using fixed values for the transmission interval and logging range, typically dictated by the maximum expected depth of the targets. Now, acoustic surveys of multiple species are conducted routinely to provide necessary information for stock assessments and to advance an ecosystem approach to fisheries management (e.g. Zwolinski *et al*, 2014). For example, NOAA Fisheries conducts annual surveys of demersal fish (Pacific whiting; aka hake) that aggregate in layers off the continental shelf to 700-m depth, requiring transmit intervals greater than ~1 s per transmission; and pelagic fishes forming small patchy school on the shelf to 70-m depth, allowing for multiple transmissions per second (e.g. Zwolinski *et al.*, 2014). As logging ranges increase to accommodate the deepest dwelling target species, transmission intervals also increase, resulting in a decrease of the achievable temporal and spatial sampling resolutions for shallower target species. Also, as the seabed rises above the logging range, unused data collected beyond the range to the seabed needlessly limit the maximum achievable sampling resolution. Furthermore, aliased seabed echoes can degrade the data quality by introducing noise and decreasing the SNR, which may require additional data processing steps and effort.

To mitigate some of these issues, the French Research Institute for Exploitation of the Sea controls their echosounders using HERMES software (Trenkel *et al.*, 2009). Based on the ER60-detected seabed depth, HERMES sets the logging range beyond the seabed and selects an associated transmit interval from a table of discrete values (L. Berger, pers. comm.). The table includes 12 candidate logging ranges between 30 and 1500 m and does not account for intermediate seabed depths. For range bins above and <250 m, the minimum transmit intervals, based on two-way pulse-travel time, are increased by empirically determined amounts to conservatively avoid the third and second seabed echoes, respectively. To avoid unacceptably large transmit intervals, this strategy is not implemented for deeper bins.

Alternatively, using the EAL, the sampling resolution and data collection may be continuously optimized for all ranges to the seabed

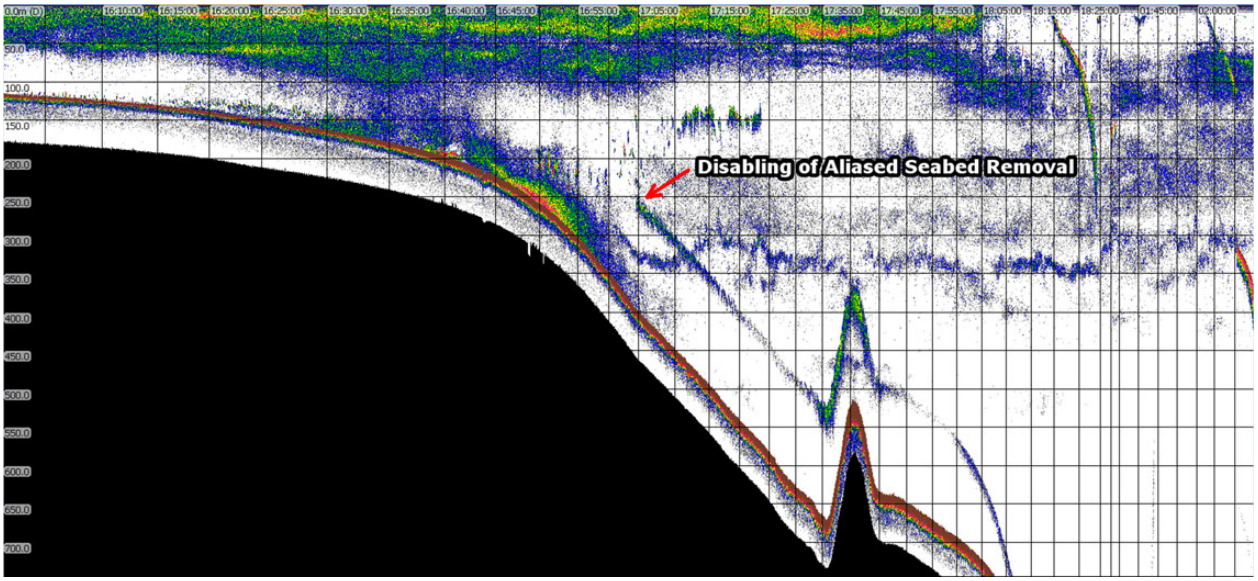

Figure 7. Eighteen kiloHertz echogram example of increased resolution, decreased data volume, and removal of aliased seabed echoes achieved using the EAL software. The number of transmissions between 5-min intervals (vertical lines) decreases as the estimated range to the seabed ($\widehat{R}_S$, m) and thus the minimum transmit-pulse interval ($I_{T\,min}$, s) increases. Samples beyond the offset range (R_0, m) below $\widehat{R}_S$ (black region) are not recorded. When $\widehat{R}_S$ is less than the maximum logging range ($R_{L\,max}$, m), an aliased seabed echo appears at ~17:05:00 at 250 m when the removal algorithm was toggled off. When R_S is greater than $R_{L\,max}$, e.g. after 18:05:00, $\widehat{R}_S$ and the aliased seabed echo range (R_{AS}, m) may be estimated using data from periodic recordings of data to depth much greater than $R_{L\,max}$ (e.g. 5 km), or by using the geographic position of the echosounder to reference $\widehat{R}_S$ from a bathymetry database. This figure is available in black and white in print and in colour at *ICES Journal of Marine Science* online.

using recently developed methods, introduced here, to accurately track the seabed depth and adapt the logging range and transmit interval. The novel algorithm avoids all aliased seabed echoes from prior transmissions and thus improves the data quality. The efficacies of these algorithms have been quantified with simulation. Furthermore, the algorithms have been collectively implemented in the EAL programme (available at https://swfsc.noaa.gov/EAL/) to improve the temporal and spatial resolution of the data, dependent on the range to the seabed and survey speed; avoid aliased seabed echoes, dependent on whether the estimated range to the seabed may be calculated from the acoustic data or referenced from a database; and reduce the volume of collected acoustic data, dependent on the amount of time the adaptive logging range is less than the chosen maximum logging range and the removal of aliased seabed echoes. The potential reductions in data volume when using adaptive logging will become increasingly significant for surveys that use wideband width or multibeam echosounders (e.g. Simrad EK80 and ME70), which can generate more than an order of magnitude additional data volume.

When multiple acoustic systems are operated concurrently, it must be emphasized to synchronize transmissions to reduce acoustic interference, typically by connecting input and output triggers between the systems or using a third-party device to supply coordinated triggers (e.g. K-sync, Simrad-Kongsberg). Currently, the EAL uses EK60 data to optimize the ER60 transmit interval, then either the ER60 provides trigger pulses to other acoustic systems or, if a synchronization system is used, the EAL provides it the optimized transmit interval information. Future versions of the EAL may use data from the EK80 to optimize the transmit interval.

For increasing f, the increase in α_a causes a decrease in observable range. Therefore, $R_{L\,max}$ and I_T could be optimized independently for each frequency, e.g. transmitting more frequently and logging to shorter ranges at higher frequencies. However, to avoid cross-talk, the aforementioned timing of all transmit pulses must be taken into account.

Although the EAL includes many contingency algorithms, e.g. to automatically restart following a temporary network malfunction, periodic supervision is recommended to ensure proper function and quality data collection.

Acknowledgements

We thank Rick Towler, Alaska Fisheries Science Center, for ER60 remote control and data subscription guidance, and Lars Nonboe Andersen from Simrad for ER60 technical support. We also thank Randy Cutter, Kevin Stierhoff, Juan Zwolinski, Steve Sessions, Dave Murfin, Scott Mau, and Brian Elliot, all from the SWFSC Advanced Survey Technologies Program, for their observations and suggestions used to refine the operational features and performance of the EAL.

References

Conti, S. G., Demer, D. A., Soule, M. A., and Conti, J. H. 2005. An improved multiple-frequency method for measuring in situ target strengths. ICES Journal of Marine Science, 62: 1636–1646.

Cutter, G. R., Jr, and Demer, D. A. 2010. Multifrequency biplanar interferometric imaging. IEEE Geoscience and Remote Sensing Letters, 7: 171–175.

Cutter, G. R., Jr, and Demer, D. A. 2014. Seabed classification using surface backscattering strength versus acoustic frequency and incidence angle measured with vertical, split-beam echosounders. ICES Journal of Marine Science, 71: 882–894.

Demer, D. A., Berger, L., Bernasconi, M., Bethke, E., Boswell, K., Chu, D., Domokos, R., *et al.* 2015. Calibration of acoustic instruments. ICES Cooperative Research Report No. 326. 133 pp.

Demer, D. A., Cutter, G. R., Jr, Renfree, J. S., and Butler, J. L. 2009. A statistical-spectral method for echo classification. ICES Journal of Marine Science, 66: 1081–1090.

Demer, D. A., Soule, M. A., and Hewitt, R. P. 1999. A multiple-frequency method for potentially improving the accuracy and precision of in situ target strength measurements. The Journal of the Acoustical Society of America, 105: 2359–2376.

Francois, R. E., and Garrison, G. R. 1982. Sound absorption based on ocean measurements. Part II: boric acid contribution and equation for total absorption. The Journal of the Acoustical Society of America, 72: 1879–1890.

MacLennan, D. N., Copland, P. J., Armstrong, E., and Simmonds, E. J. 2004. Experiments on the discrimination of fish and seabed echoes. ICES Journal of Marine Science, 61: 201–210.

Ona, E., and Mitson, R. B. 1996. Acoustic sampling and signal processing near the seabed: the deadzone revisited. ICES Journal of Marine Science, 53: 677–690.

Simmonds, J., and MacLennan, D. N. 2005. Fisheries Acoustics: Theory and Practice. Wiley-Blackwell, Oxford, UK. 456 pp.

Simrad. 2012. Simrad ER60 Scientific Echo Sounder Software Reference Manual. Kongsberg Maritime AS. 254 pp.

Trenkel, V. M., Berger, L., Bourguignon, S., Doray, M., Fablet, R., Massé, J., Mazauric, V., *et al.* 2009. Overview of recent progress in fisheries acoustics made by IFREMER with examples from the Bay of Biscay. Aquatic Living Resources, 22: 433–445.

Zwolinski, J. P., Demer, D. A., Cutter, G. R., Jr, Stierhoff, K. L., and Macewicz, B. J. 2014. Building on fisheries acoustics for marine ecosystem surveys. Oceanography, 27: 68–79.

Handling editor: Richard O'Driscoll